

Relationship of Li_2WO_4 to the scheelite tungstate scintillators: Electronic structure and atomic positions from density-functional calculations

D. J. Singh

*Materials Science and Technology Division and Center for Radiation Detection Materials and Systems,
Oak Ridge National Laboratory, Oak Ridge, Tennessee 37831-6114, USA*

(Received 22 November 2007; revised manuscript received 7 January 2008; published 4 March 2008)

Density-functional calculations of the electronic structure and atomic positions are reported for Li_2WO_4 . This compound is found to be very different from the tungstate scintillators such as PbWO_4 in that both the valence and conduction bands are much less dispersive. This leads to a substantially larger band gap. The difference is understood in terms of the crystal structure, in particular, the longer O-O distances connecting the WO_4 tetrahedra.

DOI: [10.1103/PhysRevB.77.113101](https://doi.org/10.1103/PhysRevB.77.113101)

PACS number(s): 71.20.Ps, 61.66.Fn, 29.40.Mc, 71.15.Mb

The tungstates, such as CaWO_4 , CdWO_4 , and PbWO_4 , form a useful family of inorganic scintillators. This family contains two subgroups, both based on W^{6+} : (1) scheelite-type materials, such as PbWO_4 and CaWO_4 , which are based on independent WO_4 tetrahedra separated by counterions, and (2) wolframite-type materials, such as CdWO_4 , which are based on WO_6 octahedra, with shared O ions. Despite this difference, both scheelite- and wolframite-type materials are often scintillators and, in fact, the gross features of the electronic structure are similar in the cases that have been studied.⁴⁻¹⁴ The band gaps are of charge transfer character between broad manifolds of O $2p$ valence bands and W $5d$ conduction bands.^{4,5} The local density approximation band gaps are ~ 3 eV. As is often the case, these are underestimates as compared with the experimental gaps of $\sim 4-5$ eV.¹⁰⁻¹⁴

Li_2WO_4 also forms in this case in a phenacite structure, which is a scheelite related structure based on WO_4 tetrahedra.¹⁵ Moreover, this material can be grown as large single crystals and the corresponding Mo based phase and some alloys can also be formed.¹⁶⁻¹⁸ Scintillating compounds containing large amounts of Li are of interest for thermal and low energy neutron detection. This is because of the very large cross section of ${}^6\text{Li}$ for low energy neutron capture with alpha and triton products. These reactions can be distinguished from gammas using appropriate design based on the different stopping power for the charged products and gamma rays.¹⁹

However, little is known about the relevant properties of Li_2WO_4 . Here, electronic structure calculations for Li_2WO_4 are reported in comparison with PbWO_4 , which we use as a representative scheelite-type tungstate scintillator. PbWO_4 , in particular, has become a material of choice for scintillators in high energy physics experiments due to its high stopping power, fast decay time, and other properties.¹⁻³ This material occurs in a scheelite-type tetragonal (spacegroup $I4_1/a$) structure.^{20,21} There is also a related monoclinic form.²²

The calculations were performed using the general potential linearized augmented plane wave (LAPW) method with local orbitals.^{23,24} LAPW sphere radii of $1.80 a_0$, $1.70 a_0$ and $1.45 a_0$ were used in Li_2WO_4 for W, Li, and O, respectively. For PbWO_4 , the radii were $1.85 a_0$, $2.35 a_0$, and $1.50 a_0$ for W, Pb, and O, respectively. In both cases, well converged,

tested basis sets and zone samplings were used. These consisted of ~ 7450 basis functions for Li_2WO_4 and ~ 2100 basis functions for PbWO_4 . The Brillouin zone sampling during the iteration to self-consistency was done with a set of 12 special \mathbf{k} points in the irreducible $1/6$ wedge for rhombohedral Li_2WO_4 , while the density of states was obtained with the tetrahedron method using 90 \mathbf{k} points in the wedge. For tetragonal PbWO_4 , a set of 63 special \mathbf{k} points in the irreducible $1/8$ wedge was used for self-consistency, while 78 \mathbf{k} points were used for the density of states.

The crystal structure of Li_2WO_4 , as determined by single crystal x-ray refinement,¹⁵ is phenacite ($R\bar{3}$) $a=8.888 \text{ \AA}$, $\alpha=107.78^\circ$. This structure contains 6 f.u. per cell with all atoms on general sites. There are four symmetry independent O sites and two distinct Li sites, for a total of 21 independent internal parameters.

It is very difficult to accurately determine by x-ray refinement the coordinates in structures this complex, especially considering the low atomic number of Li compared with W. Therefore, it is not surprising that large forces on the atoms were found in the local density approximation (LDA) when the experimental atomic positions were used. On the other hand, lattice parameters, as determined by x-ray diffraction, are no doubt much more accurate than can be determined within the LDA. Accordingly, the internal coordinates of the atoms were determined by total energy minimization, while the lattice parameters were held fixed at the experimental values.²⁵ This is similar to the approach used in PbZrO_3 , which yielded a structure that was confirmed by subsequent experiments.²⁶⁻²⁸ The resulting structure of Li_2WO_4 is as given in Table I and depicted in Fig. 1. We also performed a similar relaxation for scheelite PbWO_4 , starting with the low temperature structure of Ref. 21, space group $I4_1/a$, $a=5.45565 \text{ \AA}$, and $c=11.99235 \text{ \AA}$. In this structure, the only free internal parameters are associated with the O (site 16f). We obtain $x_{\text{O}}=0.2336$, $y_{\text{O}}=0.1091$, and $z_{\text{O}}=0.0415$, which is close to reported experimental values of $x_{\text{O}}=0.2388$, $y_{\text{O}}=0.1141$, and $z_{\text{O}}=0.0429$ (Ref. 20) and $x_{\text{O}}=0.2310$, $y_{\text{O}}=0.1100$, and $z_{\text{O}}=0.0425$ (Ref. 21).

The calculated electronic density of states for PbWO_4 and projections are shown in Fig. 2. It is very similar to that obtained previously by Zhang *et al.*⁴ As may be seen in the projected density of states, there is a strong W d -O p hybrid-

TABLE I. Internal atomic positions in the rhombohedral setting ($R\bar{3}$) unit cell of Li_2WO_4 . The lattice parameters, $a=8.888 \text{ \AA}$, $\alpha=107.78^\circ$, are from the experimental data of Ref. 15. All atoms are on general sites (x,y,z) , with equivalent atoms at (x,y,z) , (y,z,x) , (z,x,y) , $(\bar{x},\bar{y},\bar{z})$, $(\bar{y},\bar{z},\bar{x})$, and $(\bar{z},\bar{x},\bar{y})$. “LDA” denotes the calculated values, while “X ray” denotes the values given in Ref. 15.

	LDA			X ray		
	x	y	z	x	y	z
W	0.0338	0.4456	0.2714	0.03497	0.44606	0.27104
O1	0.1521	0.4582	0.1421	0.1505	0.4612	0.1383
O2	0.9192	0.5767	0.2494	0.9217	0.5777	0.2512
O3	0.8812	0.2210	0.1846	0.8846	0.2231	0.1902
O4	0.1869	0.5296	0.4961	0.1823	0.5263	0.4998
Li1	0.3701	0.7756	0.6098	0.386	0.782	0.605
Li2	0.7024	0.1055	0.9343	0.697	0.098	0.938

ization, as might be expected from the high valence state of W in this compound. The hybridization is evident both in the bandwidths and in the substantial admixture of W d character at the bottom of the O p bands, where the bands have t_{2g} - $p\sigma$ bonding character.

The corresponding density of states of Li_2WO_4 is shown in Fig. 3. This electronic structure is qualitatively very different from that of PbWO_4 and the other tungstate scintillators.^{4,5} As may be seen, the band gap is $\sim 2 \text{ eV}$ larger, and both the valence and conduction bands are much less dispersive, so that both the O p and W d manifolds break into separate clearly separated groups of bands corresponding to the crystal field levels. Relative to the valence band maximum, there is a very narrow peak centered at $\sim 5.2 \text{ eV}$ and another somewhat less narrow peak extending from ~ 6 to $\sim 7 \text{ eV}$. These are the crystal field split W e_g and t_{2g} manifolds, respectively. Thus, in spite of the narrowness of the bands, there is a substantial $\sim 1.5 \text{ eV}$ crystal field splitting. This is consistent with the W d character in the lower manifold of O p valence bands. Both of these features are consequences of the strong W d -O p hybridization. This is similar between PbWO_4 and Li_2WO_4 and is not surprising considering that both compounds are formed from $(\text{WO}_4)^{2-}$ units with similar bond lengths: 1.79 \AA for the relaxed structure of PbWO_4 and 1.78 – 1.79 \AA for the four inequivalent bonds in the relaxed structure of Li_2WO_4 . Also, it may be noted that the center of the O $p\pi$ states (these make up the

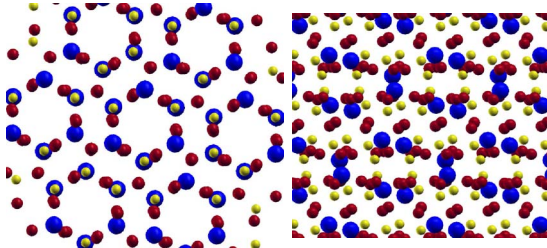


FIG. 1. (Color online) Structure of Li_2WO_4 viewed along the rhombohedral axis (left) and perpendicular to it (right). W is shown as large blue spheres, O as smaller dark red spheres, and Li as small light gold spheres.

top part of the valence bands and hybridize weakly with W d states) and the center of the W e_g states (these are the lowest crystal field level in a tetrahedral coordination and make up the bottom of the conduction bands) are separated by $\sim 6 \text{ eV}$ in both PbWO_4 and Li_2WO_4 , indicating that the difference in the on-site energy between W and O is similar in the two compounds. Thus, the big difference between the electronic structures of these two compounds is not explained by a

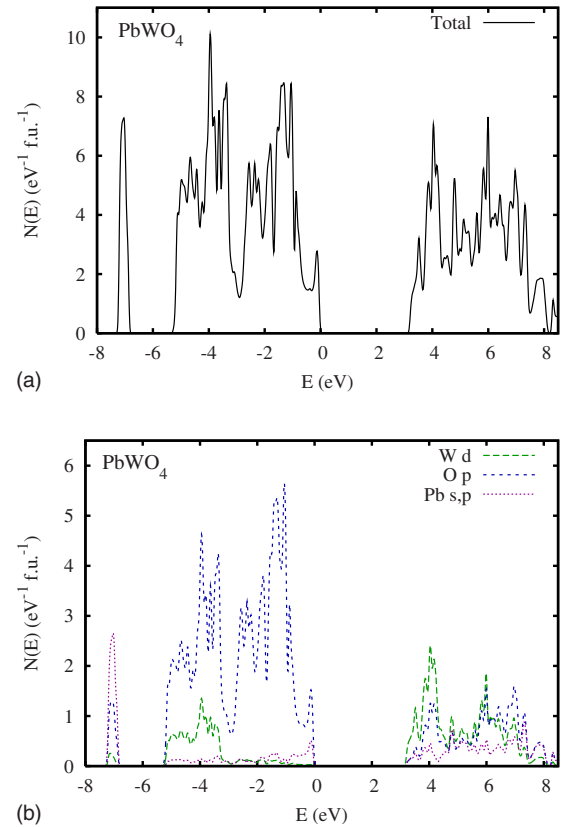


FIG. 2. (Color online) LDA density of states (top) and projections onto LAPW spheres (bottom) for PbWO_4 using the relaxed crystal structure. The valence band edge is at 0 eV . The narrow peak at $\sim -7 \text{ eV}$ is from the Pb s state. A Gaussian smoothing width of 0.04 eV was applied.

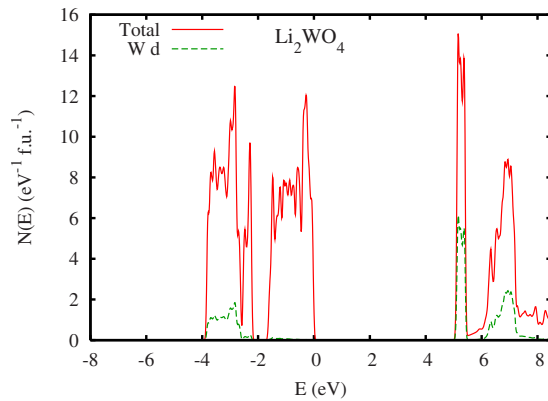


FIG. 3. (Color online) LDA density of states and W d projection onto LAPW spheres for Li_2WO_4 using the relaxed crystal structure. The Li projection (not shown) is below 0.15 eV^{-1} in the valence bands. The valence band edge is at 0 eV . A Gaussian smoothing width of 0.04 eV was applied.

difference in the p - d hybridization nor because of a difference in the relative on-site potentials of W and O. Rather, as discussed below, the difference is structural in origin.

The Pb atoms in the crystal structure of scheelite PbWO_4 are coordinated by eight O atoms, bringing O atoms belonging to different WO_4 units into proximity. This leads to short distances of 2.91 \AA between O atoms in neighboring WO_4 groups. This distance is sufficiently short to enable direct O-O hopping and explains the valence bandwidth. The W-W nearest neighbor distance is 4.11 \AA , which is much too long for direct W-W hopping. Therefore, the bandwidth in the conduction bands is from the hopping between the W via O, which again involves the same O-O bridges as for the valence bands, i.e., via an O-O distance of 2.91 \AA (note that there are no shared O atoms among the WO_4 units). These bridges form a well connected three-dimensional (3D) network of anion-anion hopping paths, as shown in Fig. 4.

The band structures of scheelite-type PbWO_4 and CaWO_4 were compared previously by Zhang *et al.*⁴ It is notable that the width of the O p bands is similar between these compounds to within $\sim 10\%$, while the conduction bands are different due to the presence of Pb $6p$ states in PbWO_4 . This is similar to that found when comparing CaMoO_4 and PbMoO_4 . This similarity argues against a strong role for the orbitals on the A-site (Ca,Pb) ion in the hopping determining the O p bandwidth.

In contrast, in Li_2WO_4 , the Li are tetrahedrally coordinated, with longer O-O distances in these tetrahedra than the short distances in PbWO_4 . The shortest distance between O of neighboring WO_4 units in Li_2WO_4 is 2.99 \AA , and these connections do not form a connected network. In order to form a 3D connected network of O-O bridges in Li_2WO_4 , it is necessary to include bond lengths up to 3.10 \AA . This is shown in Fig. 5. This difference in connectivity explains the difference between the two compounds since wave function overlaps in the tail region decrease exponentially with distance.

To summarize, the key difference between Li_2WO_4 and the tungstate scintillators is that the bands are very much

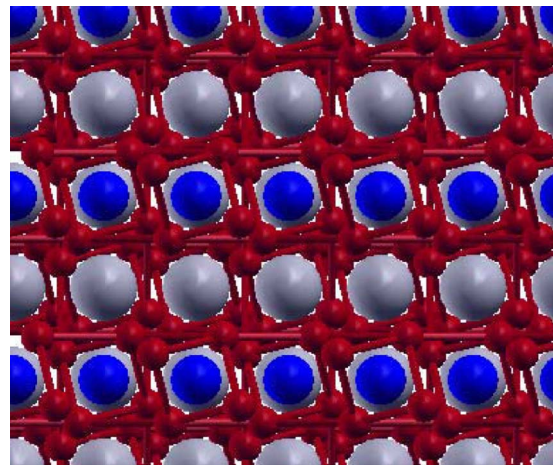


FIG. 4. (Color online) Anion network in scheelite PbWO_4 . The figure shows the structure viewed along $[010]$ (c axis is vertical, and a axis horizontal), with O depicted as small red spheres, W as medium blue spheres, and Pb as large light gray spheres. The bonds show the O-O distances of 2.91 \AA , which as shown form a connected network.

narrower in Li_2WO_4 . This difference, which leads to a larger band gap, is structural in origin. Specifically, the O-O distances connecting the WO_4 units are longer in Li_2WO_4 . While, as mentioned, the LDA underestimates the band gaps in the tungstates, the general feature of narrower bands and larger band gap due to structural differences is expected to persist.

The performance of scintillators depends on the transport of energy to the luminescent centers, which may be activator sites, such as Ce^{3+} in materials such as $\text{YPO}_3:\text{Ce}$ and $\text{LaBr}_3:\text{Ce}$, or may be intrinsic as is the case of these tungstates. The narrow bands of Li_2WO_4 will be highly detrimental to the energy transport in the form of excited carriers in this material. However, the luminescence is intrinsic in this material involving recombination of electrons in W d conduction band states with holes in the O p derived valence

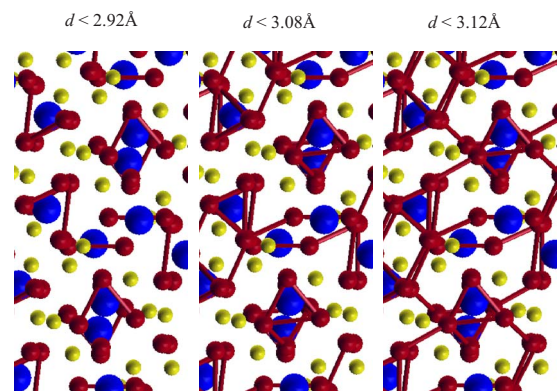


FIG. 5. (Color online) Anion network in phenacite Li_2WO_4 . The figure shows the structure, viewed close to one of the rhombohedral lattice vectors, with O depicted as small red spheres, W as larger blue spheres, and Li as the smallest gold spheres. The bonds show the O-O distances less than d for various d .

bands, both associated with the WO_4 tetrahedra.²⁹ Therefore, energy transport may not be as important as in scintillators relying on activators with percent level concentrations. In any case, while Li_2WO_4 may scintillate, it is expected to be very different in properties from the other tungstate scintillators.

I am grateful for helpful discussions with G. E. Jellison, Jr., L. A. Boatner, W. A. Shelton, Jr., Z. W. Bell, and J. S. Neal. This work was supported by the Department of Energy, Office of Nonproliferation Research and Development, NA22.

-
- ¹P. Lecoq, I. Dafinei, E. Auffray, M. Schneegans, M. V. Korzhik, O. V. Missevitch, V. B. Pavlenko, A. A. Fedorov, A. N. Annenkov, V. L. Kostylev, and V. D. Ligun, *Nucl. Instrum. Methods Phys. Res. A* **365**, 291 (1995).
- ²M. Nikl, *Phys. Status Solidi A* **178**, 595 (2000).
- ³W. W. Moses, *Nucl. Instrum. Methods Phys. Res. A* **487**, 123 (2002).
- ⁴Y. Zhang, N. A. W. Holzwarth, and R. T. Williams, *Phys. Rev. B* **57**, 12738 (1998).
- ⁵Y. Abraham, N. A. W. Holzwarth, and R. T. Williams, *Phys. Rev. B* **62**, 1733 (2000).
- ⁶Y. B. Abraham, N. A. W. Holzwarth, R. T. Williams, G. E. Matthews, and A. R. Tackett, *Phys. Rev. B* **64**, 245109 (2001).
- ⁷Y. A. Hizhnyi, S. G. Nedliko, and T. N. Nikolaenko, *Nucl. Instrum. Methods Phys. Res. A* **537**, 36 (2005).
- ⁸T. Liu, Q. Zhang, and S. Zhuang, *Phys. Lett. A* **333**, 473 (2004).
- ⁹T. Y. Liu, Q. R. Zhang, and S. L. Zhuang, *Chin. Phys. Lett.* **24**, 2361 (2007).
- ¹⁰V. Nagirnyi, E. Feldbach, L. Jönsson, M. Kirm, A. Kotlov, A. Lushchik, L. L. Nagornaya, F. Savikhin, and G. Svensson, *Radiat. Meas.* **33**, 601 (2001).
- ¹¹V. B. Mikhailik, H. Kraus, D. Wahl, M. Itoh, M. Koike, and I. K. Bailiff, *Phys. Rev. B* **69**, 205110 (2004).
- ¹²I. A. Kamenskikh, V. N. Kolobanov, V. V. Mikhailin, I. N. Shpinkov, D. A. Spassky, and G. Zimmerer, *Nucl. Instrum. Methods Phys. Res. A* **467-468**, 1423 (2001).
- ¹³I. A. Kamenskikh, V. N. Kolobanov, V. V. Mikhailin, L. I. Potkin, I. N. Shpinkov, D. A. Spassky, B. I. Zadneprovsky, and G. Zimmerer, *Nucl. Instrum. Methods Phys. Res. A* **470**, 270 (2001).
- ¹⁴A. N. Belsky, S. M. Klimov, V. V. Mikhailin, A. N. Vasilev, E. Auffray, P. Lecoq, C. Pedrini, M. V. Korzhik, A. N. Annenkov, P. Chevallier, P. Martin, and J. C. Krupa, *Chem. Phys. Lett.* **277**, 65 (1997).
- ¹⁵W. H. Zachariasen and H. A. Plettinger, *Acta Crystallogr.* **14**, 229 (1961).
- ¹⁶D. Gloeikler, F. Jeannot, and C. Gleitzer, *J. Less-Common Met.* **36**, 41 (1974).
- ¹⁷S. Yamaoka, O. Fukunaga, T. Ono, E. Iizuka, and S. Asami, *J. Solid State Chem.* **6**, 280 (1973).
- ¹⁸T. Nagasaki, S. Inui, and T. Matsui, *Thermochim. Acta* **352-323**, 81 (2000).
- ¹⁹G. F. Knoll, *Radiation Detection and Measurement*, 3rd ed. (Wiley, New York, 2000).
- ²⁰J. M. Moreau, P. Galez, J. P. Peigneux, and M. V. Korzhik, *J. Alloys Compd.* **238**, 46 (1996).
- ²¹R. Chipaux, G. Andre, and A. Cousson, *J. Alloys Compd.* **325**, 91 (2001).
- ²²T. Fujita, I. Kawada, and K. Kato, *Acta Crystallogr., Sect. B: Struct. Crystallogr. Cryst. Chem.* **B33**, 162 (1977).
- ²³D. J. Singh and L. Nordstrom, *Planewaves, Pseudopotentials and the LAPW Method*, 2nd ed. (Springer, Berlin, 2006).
- ²⁴D. Singh, *Phys. Rev. B* **43**, 6388 (1991).
- ²⁵An alternate approach would be to relax the cell parameters as well. In most cases, the error in LDA lattice parameters for $5d$ oxides is $\sim 1\% - 2\%$, which would not be expected to have a strong enough effect on the band structures to alter the conclusions presented here.
- ²⁶D. J. Singh, *Phys. Rev. B* **52**, 12559 (1995).
- ²⁷H. Fujishita and S. Katano, *J. Phys. Soc. Jpn.* **66**, 3484 (1997).
- ²⁸M. D. Johannes and D. J. Singh, *Phys. Rev. B* **71**, 212101 (2005).
- ²⁹The band gap in Li_2WO_4 is indirect with a valence band maximum at Γ and conduction band minimum along Λ . PbWO_4 also has an indirect gap, while the brighter scintillator CaWO_4 has a direct gap (Ref. 4). However, the indirect band gap of Li_2WO_4 may be less relevant because of the narrowness of the bands (the calculated difference between the direct and indirect gaps is only 0.07 eV).